Pramana – J. Phys. (2022) 96:70
https://doi.org/10.1007/s12043-022-02309-y

Gamma and neutron shielding performance of some heavy metal-incorporated borate glasses

MEHMET BEKTASOGLU[1],* and MOSLEH ALI MOHAMMAD[1,2]

[1]Department of Physics, Sakarya University, Sakarya, Turkey
[2]College of Medical and Applied Sciences, Charmo University, Chamchamal, Iraq
*Corresponding author. E-mail: mehmetb@sakarya.edu.tr

MS received 27 June 2021; revised 22 October 2021; accepted 16 November 2021

Abstract. Gamma and fast neutron shielding performances of some borate-based glasses, recently synthesised by other researchers, in the form $39H_3BO_3 + 30PbO+20MO+10Bi_2O_3+1Dy_2O_3$ (with M=Ca, Sr, Ba, Na_2 and K_2) have been investigated. The gamma shielding ability of the glasses with doped heavy metals was studied for photons with 20, 30, 40, 60, 100, 200, 284 and 511 keV energies by exploiting the mass attenuation coefficients, half-value layers, mean free paths and effective atomic numbers. It was concluded that the glass with SrO has a better shielding performance at 20 and 30 keV. For photons with energies above 30 keV, up to 511 keV, the glass having BaO is superior in terms of gamma shielding ability. Furthermore, the glass containing SrO was shown to have the best performance against fast neutrons among the glasses under investigation.

Keywords. Heavy metal-doped borate glass; FLUKA; gamma; neutron; shielding.

PACS Nos 87.53.Vb; 95.85.Pw; 87.50.Gi; 61.80.Hg

1. Introduction

Utilisation of ionising radiation has been extremely helpful in many fields including medicine, industry, agriculture and scientific research. However, usage of this powerful tool can be hazardous to human lives. This fact makes protection of the people (workers, patients etc.) mandatory against potentially harmful effects. This can be achieved using a proper shielding depending on the type and energy of the ionising radiation, in addition to reducing the time of exposure and increasing the distance to the source. Concrete is a conventional shielding material thanks to its low-cost and ability to be easily put in a desired form [1–3]. But, usage of concrete as a radiation shielding material has some drawbacks: it is not transparent to visible light and is difficult to transport. Glasses have become good candidates for radiation shielding against γ-rays and neutrons. They have significant features such as high density and resistance to corrosion, in addition to good transparency to visible light.

Many studies have been performed to investigate the performance of glasses as radiation shielding materials. Among the recent works are the ones on borate and silicate glasses containing BaO, Bi_2O_3 and PbO [4, 5], Bi_2O_3-based borate–tellurite–silicate [6], tellurite-based [7,8], lead and barium phosphate glasses [9], and Sm^{3+} [10] and Dy^{3+} [11] doped telluroborate glasses. Borate-based glasses are widely used glass systems [12–16] because B_2O_3 has a superior glass-forming ability and possesses a significantly lower melting temperature than silica glasses.

Recently, a new series of heavy metal oxides (PbO and Bi_2O_3) incorporated borate-based glasses with various modifiers such as CaO, SrO, BaO, Na_2O and K_2O and doped with the rare earth oxide Dy_2O_3, in the form of $39H_3BO_3+30PbO+20MO+10Bi_2O_3+1Dy_2O_3$ (with M = Ca, Sr, Ba, Na_2 and K_2), have been fabricated and their physical, optical and elastic properties have been investigated [17]. Some of these glasses have higher densities and refractive indices than the other recently studied Dy^{3+}-doped glasses, including zinc-aluminoborosilicate [18], alkali borotellurite [19], strontium barium borate [20] and gadolinium strontium borosilicate [21]. Response of the glasses with the different modifiers has also been studied in ref. [17] in terms of the radiation shielding performance against γ-rays of 0.284, 0.511, 0.662, 0.826, 1.172, 1.330 and 2.506 MeV energies using the Geant4 model of a high purity germanium (HPGe) detector.

Published online: 07 April 2022

In the present work, some of the main γ-ray shielding parameters for the same series of glasses analysed in [17] have been studied using the FLUKA Monte Carlo code at lower photon energies of 20, 30, 40, 60, 100, 284 and 511 keV. The first four energies, 20, 30, 40 and 60 keV, are commonly used in mammography, dental, general and computed tomography applications, respectively [22]. Mass attenuation coefficients (μ_m) have been compared with those obtained with the XCOM program. The two highest energies, namely 284 and 511 keV, are chosen to compare the μ_ms with those obtained in [17] for the same energies. In addition, the macroscopic effective removal cross-section (Σ_R) for fast neutrons has also been calculated for the glasses under study.

2. Materials and methods

Five heavy metal oxide-incorporated glasses with different modifiers fabricated in [17] have been coded in this work as:
Glass 1:
$39H_3BO_3{+}30PbO{+}20CaO{+}10Bi_2O_3{+}1Dy_2O_3$
Glass 2:
$39H_3BO_3{+}30PbO{+}20SrO{+}10Bi_2O_3{+}1Dy_2O_3$
Glass 3:
$39H_3BO_3{+}30PbO{+}20BaO{+}10Bi_2O_3{+}1Dy_2O_3$
Glass 4:
$39H_3BO_3{+}30PbO{+}20Na_2O{+}10Bi_2O_3{+}1Dy_2O_3$
Glass 5:
$39H_3BO_3{+}30PbO{+}20K_2O{+}10Bi_2O_3{+}1Dy_2O_3$.

Densities for these glasses are obtained from [17] as 5.796, 6.124, 6.260, 4.596 and 4.415 g/cm^3 for glasses 1, 2, 3, 4 and 5, respectively. The mass attenuation coefficients (μ_m) for each glass sample at 20, 30, 40, 60, 100, 200, 284 and 511 keV were calculated using the FLUKA Monte Carlo code [23–25], as well as the XCOM program [26,27]. Some of the other important shielding parameters, the half-value layers (HVL), effective atomic numbers (Z_{eff}) and mean free paths (MFP) for each glass sample have also been evaluated. Moreover, the macroscopic effective removal cross-section (Σ_R) for fast neutrons has been calculated for each glass.

2.1 *Theoretical background*

The ability of a material to be used as a shield against radiation can be estimated by means of evaluating some shielding parameters. The mass attenuation coefficient can be considered as the most significant parameter. It is defined as $\mu_m = \mu/\rho$, where ρ is the density of the target material and μ is the linear attenuation coefficient defined as

$$\mu = \frac{\ln(I_0/I)}{x}. \tag{1}$$

In this equation, obtained for a well-collimated monoenergetic photon beam, I_0 and I stand for the incident and transmitted intensities, respectively, and x is the target thickness. The mixture rule [28], given as

$$\mu/\rho = \sum_i w_i(\mu/\rho)_i, \tag{2}$$

where w_i is the fractional weight and $(\mu/\rho)_i = \mu_m$ of the ith constituent element, can be used to calculate μ_m for a mixture or a compound.

Some of the other significant radiation shielding parameters are HVL, expressed as the absorber's thickness required to decrease the gamma intensity from I_0 to $I_0/2$ (HVL $= 0.693/\mu$), the mean free path MFP $= 1/\mu$, which is the average distance taken by the incident photon before it has a collision in the absorber material and the effective atomic number Z_{eff}, which is defined for composite materials for an energy range [29]. There are various methods, such as the direct method, interpolation method, Auto-Zeff software [30] and XMuDat program [31], for calculating Z_{eff}. In the present work, the direct method has been employed. In this method, Z_{eff} is defined as the average atomic number of a compound or a mixture, given by the relation [32]

$$Z_{\text{eff}} = \frac{\sum_i f_i A_i\,(\mu/\rho)_i}{\sum_j f_i\left(A_j/Z_j\right)(\mu/\rho)_j}, \tag{3}$$

where f_i ($\sum f_i = 1$), A_i, Z_i and $(\mu/\rho)_i$ are respectively the molar fraction, atomic weight, atomic number and mass attenuation coefficient of the ith element.

The macroscopic effective removal cross-section Σ_R (in cm^{-1}) is the most significant parameter characterising attenuation of neutrons in shielding materials. It presents the probability that a fast (or fission-energy) neutron undergoes a first collision removing it from the group of penetrating uncollided neutrons [33]. For a compound or a mixture, it is defined by the relation [34]

$$\Sigma_R = \Sigma_i \rho_i (\Sigma_R/\rho)_i, \tag{4}$$

with ρ_i (g/cm^3) and $(\Sigma_R/\rho)_i$ (cm^{-1}) being the partial density and the removal cross-section per unit density of the constituent i, respectively [35]. The values of Σ_R/ρ can be calculated using the empirical functions given in [36].

2.2 *FLUKA code and XCOM program*

In this work, a fully integrated particle physics Monte Carlo simulation package, FLUKA, has been used in to obtain linear attenuation coefficients from which the

density-independent mass attenuation coefficients can be evaluated. FLUKA can calculate the particle transport and interactions of about 60 different particles, from 1 keV to thousands of TeVs, with matter [23–25]. It has many applications in cosmic ray physics, shielding, accelerator design, medical physics etc.

The XCOM program generates total cross-sections and attenuation coefficients as well as partial cross-sections for incoherent and coherent scattering, photoelectric absorption, and pair production in the fields of the atomic nucleus and atomic electrons for a wide energy range between 1 keV and 100 GeV. The interaction and total attenuation coefficients for compounds or mixtures are obtained as sums of the corresponding quantities for the atomic constituents. XCOM calculates the weighting factors, the fractions by weight of the constituents from the chemical formula entered by the user. In the case of mixtures, the fractions by weight of the various components must be given by the user [26,27].

3. Results and discussion

The first step to calculate the mass attenuation coefficients using FLUKA is to obtain the linear attenuation coefficient using eq. (1). To achieve that goal, the targets representing the glasses have been formed as a rectangular box of 4 cm height, 4 cm width and a variable thickness t. Each target has been constructed in the form $39H_3BO_3{+}30PbO{+}20MO{+}10Bi_2O_3{+}1Dy_2O_3$ where M is replaced by Ca, Sr, Ba, Na_2 and K_2 to make different glasses. The weight fraction of each element in the individual glass is given in table 1. Simulations have been performed for each glass by delivering 5×10^5 mono-energetic gamma photons with the energy of interest, namely 20, 30, 40, 60, 100, 200, 284 and 511 keV, perpendicular to the target. At each energy, simulations have been repeated with the target having different thicknesses and the transmitted photon intensities have been recorded for each case. For each glass and photon energy of interest μ is extracted from a fit to the function $y = ax + b$ where x is the target thickness and $y = \ln(I/I_0)$. The mass attenuation coefficients of the glasses (μ_m) are then obtained by dividing μ by the density of the corresponding glass.

Results acquired from the simulations and XCOM, together with the percentage difference (PD) calculated using the equation

$$\mathrm{PD} = \frac{|\mu_{m(\mathrm{XCOM})} - \mu_{m(\mathrm{FLUKA})}|}{\mu_{m(\mathrm{XCOM})}} \times 100 \qquad (5)$$

are given in tables 2 and 3.

It is clear from tables 2 and 3 that FLUKA successfully reproduces the mass attenuation coefficients obtained with XCOM, with the smallest percentage difference of 0.02% for Glass 2 at 30 keV photon energy and the largest one of 0.95% for Glass 4 at 200 and 511 keV photon energies. It is noteworthy to compare the μ_m values obtained from FLUKA with those obtained using the Geant4 simulation toolkit reported in [17]. Since this work mainly focusses on relatively low energies, comparison can be made between the FLUKA and Geant4 μ_m values at 284 and 511 keV photon energies. It has been reported [17] that Geant4 results for μ_m are 0.3474, 0.3351, 0.3327, 0.3416 and 0.3312 (0.1315, 0.1295, 0.1302, 0.1312 and 0.1294) cm^2/g at 284 (511) keV for Glass 1, 2, 3, 4 and 5, respectively. The percentage differences calculated between each of these values and the corresponding XCOM ones are obtained to be greater than 1% (reaching 3.45% for Glass 1 at 511 keV) for almost all the values, except for Glass 1 at 284 keV.

The μ_m values obtained using the FLUKA code have also been depicted in figure 1 for all the energies under investigation. The region representing the medical diagnostic energies 20, 30, 40 and 60 keV is zoomed and embedded in the figure as well. One can notice from table 2 and figure 1 that the mass attenuation coefficients suddenly decrease as the photon energy increases from 20 to 60 keV. This behaviour clearly indicates that the shielding ability of all the glasses sharply decreases with the increase in photon energy. Furthermore, Glass 2, which contains SrO, has the largest mass attenuation coefficient compared to the other glasses at 20 and 30 keV photon energies. This can be attributed to the fact that Sr has the K absorption edge at 16.1 keV, which is the energy equal to the binding energy of the innermost shell of Sr atoms. Gamma rays with such energies attenuated strongly due to the photoelectric absorption causing a sharp increase in the mass attenuation coefficient. This phenomenon, which is effective at 20 keV and to a lesser extent at 30 keV, gradually decreases as the photon energy increases. At 40 keV and 60 keV, Glass 3 has the largest μ_m among the other glasses. The situation can be explained in a similar manner as above: Glass 3 with its barium content shows better shielding performance against photons at 40 KeV and to a lesser extent 60 keV due to its K absorption edge at 37.4406 keV. At the higher set of energies, namely 100, 200, 284 and 511 keV, the μ_m values continue to decrease, except for a slight increase at 100 keV, until they reach the lowest value at 511 keV.

The half value layer (HVL) is another parameter by which the photon shielding ability of a material can be estimated. Since it gives the thickness of the target material that can decrease gamma intensity to 50% of the incident intensity, lower values of HVL mean better protection against γ-rays. The HVLs of the glasses under

Table 1. Weight fraction of the elements in the glasses.

Glass samples	Weight fractions						
	B	Pb	Bi	Dy	O	H	Ca/Sr/Ba/Na/K
Glass 1	0.02762678	0.40729660	0.27386421	0.02129527	0.20966863	0.00772717	0.05252134 (Ca)
Glass 2	0.02600650	0.38340915	0.25780241	0.02004633	0.19737183	0.00727398	0.10808980 (Sr)
Glass 3	0.02450393	0.36125703	0.24290744	0.01888812	0.18596833	0.00685371	0.15962144 (Ba)
Glass 4	0.02741476	0.40417080	0.27176245	0.02113184	0.20805954	0.00766787	0.05979275 (Na)
Glass 5	0.02631238	0.38791867	0.26083459	0.02028211	0.19969324	0.00735953	0.09759949 (K)

Table 2. Mass attenuation coefficients (μ_m) in cm^2/g obtained with FLUKA and XCOM for the glasses under study at medical diagnostic energies.

	20 keV			30 keV			40 keV			60 keV		
GS	FLUKA	XCOM	PD (%)	FLUKA	XCOM	PD (%)	FLUKA	XCOM	PD (%)	FLUKA	XCOM	PD (%)
Glass 1	61.21118	61.59	0.62	21.6563	21.63	0.12	10.2112	10.26	0.48	3.7995	3.827	0.72
Glass 2	63.81940	64.23	0.64	22.4935	22.49	0.02	10.5838	10.63	0.43	3.8937	3.918	0.62
Glass 3	58.42173	58.71	0.49	20.5048	20.57	0.32	12.8883	12.94	0.40	4.7105	4.722	0.24
Glass 4	60.31549	60.56	0.40	21.2132	21.29	0.36	10.0711	10.11	0.38	3.7742	3.777	0.08
Glass 5	58.81279	59.07	0.44	20.6689	20.73	0.29	9.7976	9.833	0.36	3.6582	3.668	0.27

Table 3. Mass attenuation coefficients (μ_m) in cm^2/g obtained with FLUKA and XCOM for glasses under study at 100, 200, 284 and 511 keV photon energies.

	100 keV			200 keV			284 keV			511 keV		
GS	FLUKA	XCOM	PD (%)	FLUKA	XCOM	PD (%)	FLUKA	XCOM	PD (%)	FLUKA	XCOM	PD (%)
Glass 1	3.9279	3.955	0.69	0.7345	0.7406	0.83	0.34928	0.35	0.63	0.1359	0.1362	0.23
Glass 2	3.7778	3.801	0.61	0.7105	0.7124	0.27	0.33908	0.3395	0.12	0.1319	0.1329	0.76
Glass 3	3.8173	3.846	0.75	0.7168	0.715	0.25	0.33789	0.3395	0.47	0.1323	0.1322	0.10
Glass 4	3.9062	3.921	0.38	0.7279	0.7349	0.95	0.34706	0.3492	0.61	0.1343	0.1356	0.95
Glass 5	3.7675	3.777	0.25	0.7110	0.7113	0.04	0.33730	0.3399	0.77	0.1329	0.1337	0.57

study at the energies of interest are plotted in figure 2. In the figure is embedded the zoomed region representing the HVLs for the medical diagnostic energies. The first observation from the figure is that Glasses 4 and 5 have the largest HVL values for all energies of interest. This means Glasses 4 and 5 have the weakest shielding ability. Secondly, one can see from the embedded figure that Glass 2 has the smallest HVL at 20 and 30 keV, after which Glass 3 has the lowest HVL value. This observation implies that while Glass 2 exhibits better shielding ability at 20 and 30 keV, Glass 3's shielding performance becomes better than the other glasses for energies above 30 keV.

The mean free paths (MFP) of the glasses are given in figure 3 as a function of the photon energy. Owing to the fact that the MFP is closely related to the linear attenuation coefficient by the relation MFP $= 1/\mu$, the energy dependence of MFP is very similar to that of HVL. Therefore, the conclusions drawn from the HVL are valid for the MFP. Glass 2, with the smallest value of MFP, has better shielding capacity at 20 and 30 keV. Glass 3 has the best shielding performance for photon energies above 30 keV.

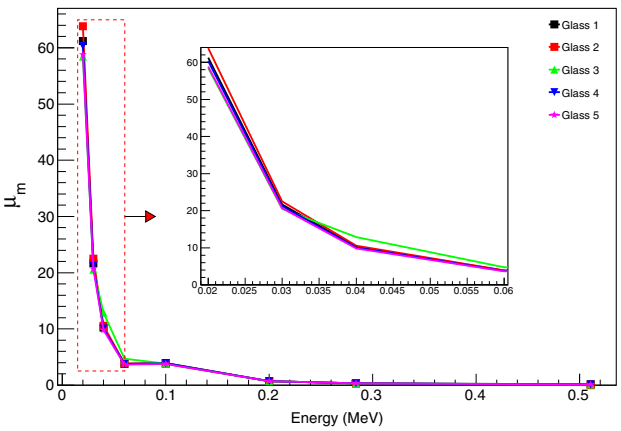

Figure 1. μ_m values obtained with FLUKA for the glasses under study at photon energies of interest.

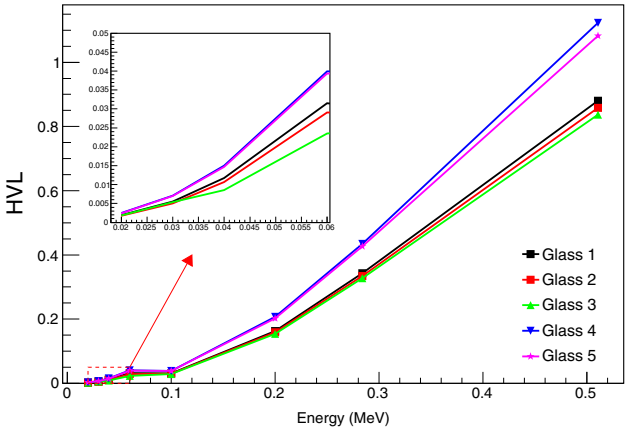

Figure 2. Dependence of the HVL of the glasses on photon energy.

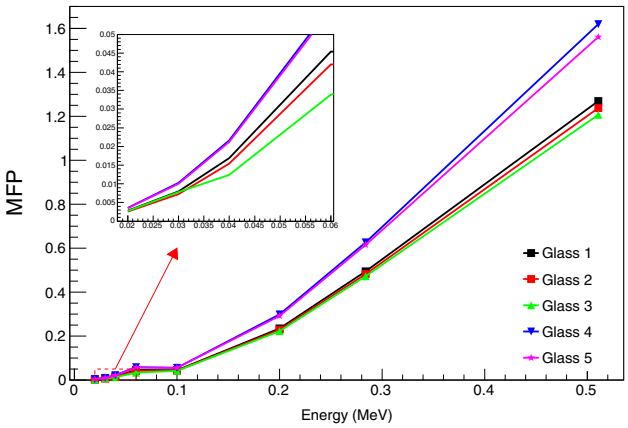

Figure 3. Dependence of the MFP of the glasses on photon energy.

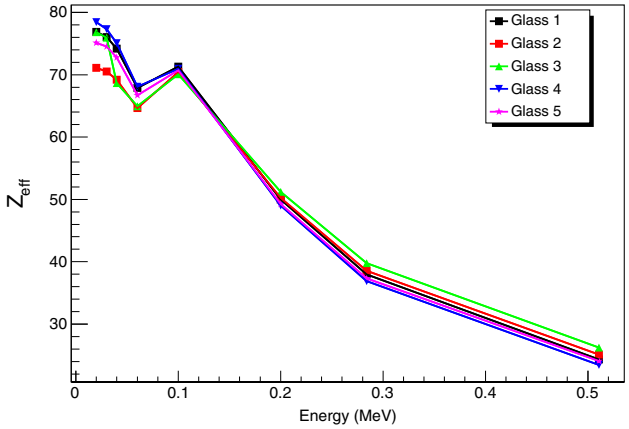

Figure 4. Dependence of Z_{eff} of the glass samples as a function of photon energy.

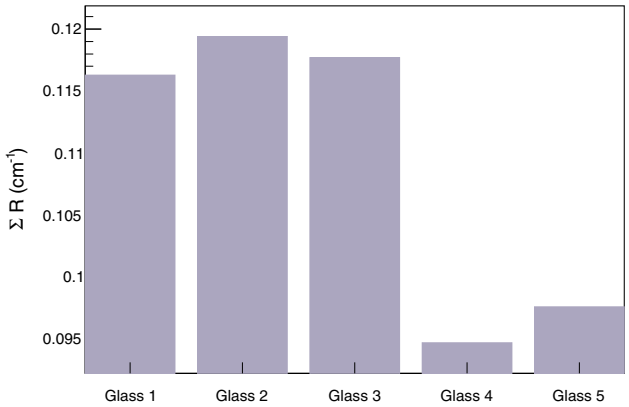

Figure 5. Fast neutron removal cross-sections for the glass samples under study.

The effective atomic numbers (Z_{eff}) for the glass samples as a function of photon energies of interest are given in figure 4. It is well-known that high values of Z_{eff} means better shielding against photons since the photoelectric absorption is approximately proportional to the third power of the atomic number. From figure 4, it is seen that Z_{eff} sharply decreases when the photon energy increases from 20 keV to 60 keV after which Z_{eff} slightly increases with the increase in the photon energy up to 100 keV for all the glasses under study. After 100 keV, Z_{eff} again decreases as the photon energy increases. For photon energies above ∼130 keV up to 511 keV, Z_{eff} is the largest for Glass 3 and the smallest for Glass 4. This may mean that Glass 3 (Glass 4), among the glasses of interest, has the best (worst) shielding ability against photons in this energy region. These observations are consistent with those made with the HVL and MFP calculations. On the other hand, for energies below 100 keV, there seems to be a discrepancy between the conclusions made using Z_{eff} and those of the other parameters, namely μ_m, HVL and MFP. This discrepancy can be due to the fact that the Z_{eff} values are sensitive to the method used in the calculations in the energy range where the photoelectric absorption dominates [37,38].

The macroscopic effective removal cross-sections (Σ_R) have been evaluated for the glasses under study and the results are depicted in figure 5. Table 4 includes the weight fractions (WF), partial densities (PD) and microscopic removal cross-sections for the individual constituents in addition to the macroscopic effective removal cross-sections given in figure 5. The letter 'X' in the table stands for Ca, Sr, Ba, Na and K for Glasses 1, 2, 3, 4 and 5, respectively. As seen from both figure 5 and table 4, Σ_R(Glass 2) > Σ_R(Glass 3) > Σ_R(Glass 1) > Σ_R(Glass 5) > Σ_R(Glass 4). One may conclude from these results that Σ_R is affected both by the density of the glass and the weight fraction of the elements having low atomic number, and that Glass 2 (Glass 4), with its largest (lowest) Σ_R, has the best (worst) shielding ability against fast neutrons among the glasses under investigation.

Table 4. Σ_R (cm^{-1}) for the glasses under study.

		Element							Total
		B	Pb	Bi	Dy	O	H	X	Σ_R (cm^{-1})
Glass 1	WF (%)	0.0276	0.4073	0.2739	0.0213	0.2097	0.0077	0.0525	
	PD (g/cm^3)	0.15997	2.36071	1.58752	0.12345	1.21542	0.04463	0.30429	
	Σ_R (cm^{-1})	0.0092	0.0246	0.0164	0.0014	0.0492	0.0085	0.0070	0.1163
Glass 2	WF (%)	0.0260	0.3834	0.2578	0.0200	0.1974	0.0073	0.1081	
	PD (g/cm^3)	0.15922	2.34794	1.57877	0.12248	1.20888	0.04471	0.662	
	Σ_R (cm^{-1})	0.0092	0.0244	0.0163	0.0014	0.0490	0.0085	0.0106	0.1194
Glass 3	WF (%)	0.0245	0.3613	0.2429	0.0189	0.1860	0.0069	0.1596	
	PD (g/cm^3)	0.15337	2.26174	1.52055	0.11831	1.16436	0.04319	0.9991	
	Σ_R (cm^{-1})	0.0088	0.0235	0.0157	0.0014	0.0472	0.0082	0.0129	0.1177
Glass 4	WF (%)	0.0274	0.4042	0.2718	0.0211	0.2081	0.0077	0.0598	
	PD (g/cm^3)	0.12593	1.8577	1.24919	0.09698	0.95643	0.03539	0.27484	
	Σ_R (cm^{-1})	0.0072	0.0193	0.0129	0.0011	0.0387	0.0067	0.0088	0.0947
Glass 5	WF (%)	0.0263	0.3879	0.2608	0.0203	0.1997	0.0074	0.0976	
	PD (g/cm^3)	0.12671	1.8689	1.25653	0.09781	0.96215	0.03565	0.47024	
	Σ_R (cm^{-1})	0.0073	0.0194	0.0129	0.0011	0.0390	0.0068	0.0111	0.0976

4. Conclusions

The ability of the glasses in the form $39H_3BO_3$+ $30PbO$+$20MO$+$10Bi_2O_3$+$1Dy_2O_3$, where M stands for Ca, Sr, Ba, Na_2 and K_2, to shield against photons with energies 20, 30, 40, 60, 100, 200, 284 and 511 keV has been investigated by determining various radiation shielding parameters. The mass attenuation coefficients obtained using the FLUKA Monte Carlo program have been compared with those of the XCOM program; the results of the two programs are found to be consistent with each other. The HVL, MFP and Z_{eff} values have been also been calculated. We conclude that Glass 2, with SrO content, has better shielding capacity at 20 and 30 keV, while Glass 3, with BaO, has the best shielding performance for photon energies above 30 keV. Furthermore, the shielding performance of the glasses against fast neutrons has been studied by calculating the macroscopic effective removal cross-sections (Σ_R), and it has been shown that Glass 2 has the best performance among the glasses under investigation.

References

[1] E Yılmaz, H Baltas, E Kırıs, I Ustabas, U Cevik and A M El-Khayatt, *Ann. Nucl. Energy* **38**, 2204 (2011)

[2] A W El-Sayed and M A Bourham, *Ann. Nucl. Energy* **85**, 306 (2015)

[3] G Tyagi, A Singhal, S Routroy, D Bhunia and M Lahoti, *J. Hazard. Mater.* **404**, 124201 (2021)

[4] R Bagheri and S P Shirmardi, *Radiat. Phys. Chem.* **184**, 109434 (2021)

[5] K Kirdsiri, J Kaewkhao, N Chanthima and P Limsuwan, *Ann. Nucl. Energy* **38**, 1438 (2011)

[6] S A M Issa and A M A Mostafa, *J. Alloys Compd.* **695**, 302 (2017)

[7] M Y Hanfi, M I Sayyed, E Lacomme, I Akkurt and K A Mahmoud, *Nucl. Eng. Technol.* **53(6)**, 2000 (2021)

[8] M Bektasoglu and M A Mohammad, *Ceram. Int. B* **46(10)**, 16217 (2020)

[9] M H Kharita, R Jabra, S Yousef and T Samaan, *Radiat. Phys. Chem.* **81(10)**, 1568 (2012)

[10] R Divina, K Marimuthu, M I Sayyed, H O Tekin and O Agar, *Radiat. Phys. Chem.* **160**, 75 (2019)

[11] R Divina, K Marimuthu, K A Mahmoud and M I Sayyed, *Ceram. Int.* **46**, 17929 (2020)

[12] Y S Alajerami, D A Drabold, M H A Mhareb, K N Subedi, K L A Cimatu and G Chen, *J. Appl. Phys.* **127(17)**, 175102 (2020)

[13] M H A Mhareb, M Alqahtani, F Alshahri, Y S M Alajerami, N Saleh, N Alonizan, M I Sayyed, M G B Ashiq, T Ghrib, S I Al-Dhafar, T Alayed and M A Morsy, *J. Non-Cryst. Solids* **541**, 120090, (2020)

[14] G Lakshminarayana, S O Baki, K M Kaky, M I Sayyed, H O Tekin, A Lira, I V Kityk and M A Mahdi, *J. Non-Cryst. Solids* **471**, 222 (2017)

[15] M S Al-Buriahi, Y S M Alajerami, A S Abouhaswa, A Alalawi, T Nutaro and B Tonguc, *J. Non-Cryst. Solids* **544**, 120171 (2020)

[16] A S Abouhaswa, M I Sayyed, A S Altowyan, Y Al-Hadeethi and K A Mahmoud, *Opt. Mater.* **106**, 109981 (2021)

[17] D Raj, S Priya, K Marimuthu, A Askin and M I Sayyed, *J. Non-Cryst. Solids* **545**, 120269 (2020)

[18] M Monisha, A N D'Souza, V Hegde, N S Prabhu, M I Sayyed, G Lakshminarayana and S D Kamath, *Curr. Appl. Phys.* **20**, 1207 (2020)

[19] P E Teresa, K A Naseer, K Marimuthu, H Alavian and M I Sayyed, *Radiat. Phys. Chem.* **189**, 109741 (2021)
[20] G Sathirapriya, K A Naseer, K Marimuthu, E Kavaz, A Alalawi and M S Al-Buriahi, *J. Mater. Sci.: Mater. Electron.* **32**, 8570 (2021)
[21] K Mariselvam, J Liu and H Chen, *Mater. Chem. Phys.* **263**, 124421 (2021)
[22] Australian Radiation Protection and Nuclear Safety Agency (ARPANSA), https://www.arpansa.gov.au/
[23] T T Böhlen, F Cerutti, M P W Chin, A Fassò, A Ferrari, P G Ortega, A Mairani, P R Sala, G Smirnov and V Vlachoudis, *Nucl. Data sheets* **120**, 211 (2014)
[24] A Ferrari, P R Sala, A Fasso and J Ranft, *FLUKA: a multi-particle transport code* (CERN-2005-10)
[25] *The official FLUKA site: FLUKA home*. http://www.fluka.org
[26] M J Berger and J H Hubbell, National Bureau of Standards, Washington, DC, USA, Center for Radiation Research (1987)
[27] M J Berger, J H Hubbell, S M Seltzer, J Chang, J S Coursey, R Sukumar, D S Zucker and K Olsen, *NIST, PML, Radiation Physics Division* (2010)
[28] D F Jackson and D J Hawkes, *Phys. Rep.* **70(3)**, 169 (1981)
[29] G J Hine, *Phys. Rev.* **85**, 725 (1952)
[30] M L Taylor, R L Smith, F Dossing and R D Franich, *Med. Phys.* **39(4)**, 1769 (2012)
[31] R Nowotny, IAEA-NDS **195**, 52 (1998)
[32] S R Manohara, S M Hanagodimath, K S Thind and L Gerward, *Nucl. Instrum. Methods Phys. Res. B* **266(18)**, 3906 (2008)
[33] A B Chilton, J K Shultis and R E Faw, *Principles of radiation shielding* (Prentice Hall Inc., United States, 1984)
[34] M F Kaplan, *Concrete radiation shielding: Nuclear physics, concrete properties, design and construction* (Longman Scientific & Technical, 1989)
[35] F A R Schmidt, *Nucl. Eng. Des.* **10(3)**, 308 (1969)
[36] L K Zoller, *Nucleonics (US) Ceased publication* **22** (1964)
[37] S R Manohara, S M Hanagodimath and L Gerward, *Med. Phys.* **36(1)**, 137 (2009)
[38] V P Singh, N M Badiger and N Kucuk, *J. Nucl. Chem.* **2014**, 1 (2014)